nature materials
SUPPLEMENTARY INFORMATION
https://doi.org/10.1038/s41563-018-0118-1
In the format provided by the authors and unedited.

Coupling two order parameters in a quantum gas

Andrea Morales[1], Philip Zupancic[1], Julian Léonard[1,2], Tilman Esslinger[1]* and Tobias Donner[1]

[1]Institute for Quantum Electronics, ETH Zurich, Zurich, Switzerland. [2]Department of Physics, Harvard University, Cambridge, MA, USA.
*e-mail: esslinger@phys.ethz.ch

Supplementary Information for Coupling two order parameters in a quantum gas

Andrea Morales,[1] Philip Zupancic,[1] Julian Léonard,[1,2] Tilman Esslinger,[1,*] and Tobias Donner[1]

[1]*Institute for Quantum Electronics, ETH Zurich, 8093 Zurich, Switzerland*
[2]*Department of Physics, Harvard University, Cambridge, Massachusetts 02138, USA.*

Excitation spectrum To measure the excitation spectrum we exploit a method which we have introduced in a previous work [1]. We first fix the cavity detunings from the pump laser frequency to certain values $(\Delta_1^{\mathrm{eq}}, \Delta_2^{\mathrm{eq}})$. We then prepare the BEC at a certain coupling strength by linearly increasing the transverse pump intensity within 50 ms to a lattice depth of $12.5(10)\,\hbar\omega_{\mathrm{rec}}$, with ω_{rec} being the recoil frequency for a transverse pump photon. This brings the system to a certain position in the phase diagram where we want to probe the excitations. Subsequently, a small probe field is injected on axis with one of the cavity modes and its detuning is ramped linearly in time from 0 kHz to 6 kHz with respect to the transverse pump frequency within 20 ms. Simultaneously, we measure the response of the system to the probe field by continuously monitoring the number of photons leaking from the cavity mirrors on single photon detectors. We bin photons in 0.25 ms intervals, apply a smoothing filter and average 20 traces for each position in the phase diagram. Fig. 1 shows an examplary measurement.

Hamiltonian description of the system Raman scattering between the cavity fields (with wave-vector $\mathbf{k}_i$, $i \in \{1, 2\}$) and the transverse pump (with wave-vector $\mathbf{k}_{\mathrm{p}}$) via the atoms couples the atomic momentum state of the BEC to a superposition state of higher momenta. These states fall into two groups with energies either $\hbar\omega_- = \hbar\omega_{\mathrm{rec}}$ or $\hbar\omega_+ = 3\hbar\omega_{\mathrm{rec}}$ (see Fig. 3). The single-photon recoil frequency is given by $\omega_{\mathrm{rec}} = \hbar k^2/2m$, with m being the atomic mass and $\hbar$ the reduced Planck constant and $k = |\mathbf{k}_{\mathrm{p}}| = |\mathbf{k}_i|$. Following the same

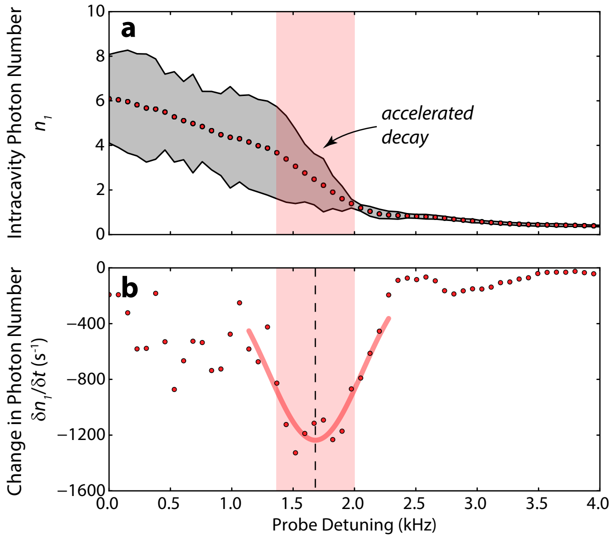

FIG. 1. **Measurement of the excitation energy.** The figure illustrates the measurement for the case of $\Delta_1/2\pi = -4\,\mathrm{MHz}$, $\Delta_2/2\pi = -4.75\,\mathrm{MHz}$, i.e. $\bar{\Delta}/2\pi = 0.75\,\mathrm{MHz}$, measured on cavity 1. **a,** Order parameter n_1 responding to the weak probe field whose detuning is changing from 0 kHz to 4 kHz with respect to the transverse pump frequency within 20 ms. The data is binned in 0.25ms intervals, smoothened, and averaged over 20 realizations. The gray shaded area shows the standard deviation of the full sample. The red shaded area highlights the region of accelerated decay. **b,** The time derivative of the mean photon trace shows a resonance at a detuning of 1.7 kHz (dashed line). A collective mode is excited at this frequency, which subsequently decays. The excess energy of the decay leads to heating which we observe through the decreasing order parameter. We extract the resonance frequency with a local Gaussian fit (light red).

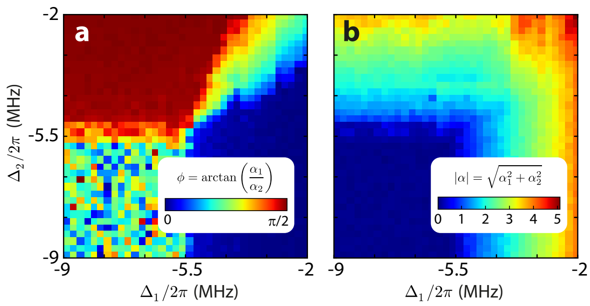

FIG. 2. **Phase and amplitude of the order parameter.** The data from Fig. 2 of the main text is transformed into the phase $\phi = \arctan(\alpha_1/\alpha_2)$ (**a**) and amplitude $|\alpha| = \sqrt{\alpha_1^2 + \alpha_2^2}$ (**b**) of the composite order parameter. The phase is random in the non-ordered phase ($\Delta_1/2\pi, \Delta_2/2\pi < -5.5\,\mathrm{MHz}$), fixed at 0 or $\pi/2$ in the singly self-organized phase of cavity 1 or 2 respectively, and smoothly varying between them in the mixed phase.

procedure described in the Methods section of [2], we include the cavity–cavity interference term and extend the ansatz for the atomic field operator to

$$
\begin{aligned}
\hat{\Psi} =&\Psi_0\hat{c}_0 + \sum_{i\in\{1,2\}} \left(\Psi_{i-}\hat{c}_{i-} + \Psi_{i+}\hat{c}_{i+}\right) \\
&+ \Psi_{12-}\hat{c}_{12-} + \Psi_{12+}\hat{c}_{12+},
\end{aligned}
\tag{1}
$$

where $\hat{c}^\dagger_{i\pm}$ ($\hat{c}_{i\pm}$) and $\hat{c}^\dagger_0$ ($\hat{c}_0$) create (annihilate) an atomic momentum excitation at energy $\hbar\omega_\pm$ associated with cavity i and in the atomic ground state, respectively. $\hat{c}^\dagger_{12\pm}$ ($\hat{c}_{12\pm}$) create (annihilate) an atomic momentum excitation at energy $\hbar\omega_\pm$ associated to cavity–cavity scattering. $\Psi_0 = \sqrt{\frac{2}{A}}$ represents the BEC zero-momentum mode, the functions $\Psi_{i\pm} = \sqrt{\frac{2}{A}}\cos[(\mathbf{k}_\mathrm{p} \pm \mathbf{k}_i)\cdot\mathbf{r}]$ are the atomic modes with momentum imprinted by one of the scattering processes at high– or low–energy into one of the cavities, and the functions $\Psi_{12\pm} = \sqrt{\frac{2}{A}}\cos[(\mathbf{k}_1 \mp \mathbf{k}_2)\cdot\mathbf{r}]$ are the atomic modes with momentum imprinted by one of the scattering processes at high– or low–energy from one cavity to the other. $\mathbf{r}$ is the real space coordinate vector and A is the area of the Wigner-Seitz cell. We obtain the following effective Hamiltonian

$$
\begin{aligned}
\hat{\mathcal{H}} = \sum_{i\in\{1,2\}} \Big[&-\hbar\Delta_i\hat{a}^\dagger_i\hat{a}_i + \hbar\omega_+\hat{c}^\dagger_{i+}\hat{c}_{i+} + \hbar\omega_-\hat{c}^\dagger_{i-}\hat{c}_{i-} \\
&+ \frac{\hbar\lambda_i}{\sqrt{N}}\left(\hat{a}^\dagger_i + \hat{a}_i\right)\left(\hat{c}^\dagger_{i+}\hat{c}_0 + \hat{c}^\dagger_{i-}\hat{c}_0 + h.c.\right)\Big] \\
&+ \frac{\hbar\lambda_{12}}{\sqrt{N}}\left(\hat{a}^\dagger_1\hat{a}_2 + \hat{a}^\dagger_2\hat{a}_1\right)\left(\hat{c}^\dagger_{12-}\hat{c}_0 + \hat{c}^\dagger_{12+}\hat{c}_0 + h.c.\right) \\
&+ \hbar\omega_-\hat{c}^\dagger_{12-}\hat{c}_{12-} + \hbar\omega_+\hat{c}^\dagger_{12+}\hat{c}_{12+},
\end{aligned}
\tag{2}
$$

where the index i labels the two cavities and N is the atom number. $\hat{a}^\dagger_i$ ($\hat{a}_i$) are the creation (annihilation) operators for a photon in cavity i. $\lambda_i = \frac{\eta_i\sqrt{N}}{2\sqrt{2}}$ is the Raman coupling between the transverse pump and cavity i, which can be controlled via $\eta_i = -\frac{\Omega_\mathrm{p}g_i}{\Delta_a}$ with the transverse pump Rabi frequency Ω_p. $\lambda_{12} = -\frac{g_1 g_2 N}{2\sqrt{2}\Delta_\mathrm{A}}$ is the Raman coupling between one cavity and the other one and can be controlled via the atomic detuning Δ_A. The atomic cloud acts as a dispersive medium in the cavity and changes the effective cavity lenght. The resulting dispersive shift of the cavity resonance is $Ng_i^2/(2\Delta_a) \ll \Delta_i$. It is similar for both cavities and we absorbe it into Δ_i. Higher order terms can be discarded for our experimental parameters. For our experimental parameters, collisional interactions between the atoms result only in a small overall energy shift. Since the vacuum Rabi couplings g_i of the two cavities are slightly different, the BEC is aligned at the position where we achieve equal effective vacuum Rabi couplings $\tilde{g}_i$ of the two cavities due to the convolution with the mode profiles of the cavities. This position is slighlty off centered with respect to the mode crossing but ensures that we can use $g_0 = \tilde{g}_1 = \tilde{g}_2$ and a single coupling $\lambda = \lambda_1 = \lambda_2$. In the most general case of two coupled order parameters the free energy coefficients g_1 and g_2 would be different. In our experiment we can change these coefficients by placing the BEC at a position that has a larger overlap with one of the two cavity modes. We neglect the cavity decay rates which are not relevant in this part of the discussion. We also neglect effects due to the spatial phase of the transverse pump lattice relative to the cavity lattices.

Symmetries and phases The Hamiltonian (2) possesses two $\mathbb{Z}_2$ symmetries that can be broken independently. When photons are coherently scattered from the transverse pump into either of the cavities, a light field amplitude α_i in cavity i becomes non-zero and can take either 0 or π phase with respect to the transverse pump beam phase, as the electric field has to match the boundary conditions set by the cavity mirror. These two phases of the light field correspond in real space to atoms sitting on even or odd sites of the interference potential that is formed between the transverse pump beam and the cavity lattice.

Low-energy mean field expansion Here we show an exact mapping of our microscopic

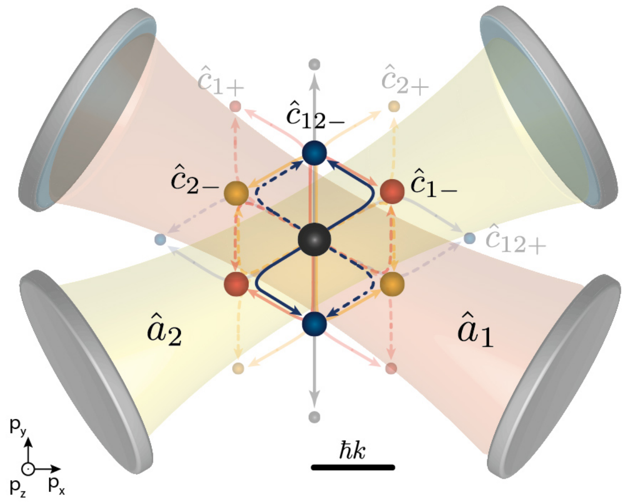

FIG. 3. **Field operators describing the scattering processes.** The cavity modes, with photon annihilation operators $\hat{a}_1$ and $\hat{a}_2$, are sketched in red and yellow. Red (yellow) circles are atomic momentum states populated via photon scattering from the pump into cavity 1 (cavity 2) and vice versa. The associated annihilation operators are $\hat{c}_{1\pm}$ and $\hat{c}_{2\pm}$ respectively. Blue circles are atomic momentum states occupied via photon scattering from one cavity to the other, associated with the annihilation operator $\hat{c}_{12\pm}$. Black circles represent the BEC state and the Bragg peaks of the transverse pump lattice oriented along y. The momentum peaks in darker colour have energy $\hbar\omega_-$ whereas those in transparency have higher energy $\hbar\omega_+$ and are neglected in the derivation of the free energy. The scale $\hbar k$ indicates the atomic recoil momentum given by a pump photon. Solid and dahed lines correspond to different time ordered two-photon scattering processes.

model on a Landau free energy that captures the phenomenology of the phase diagram of two coupled order parameters. Starting from the Hamiltonian $\hat{\mathcal{H}}$ we restrict our description to the low-energy momentum modes $\hbar\omega_-$ which are highlighted in Fig. 3:

$$\begin{aligned}\hat{\mathcal{H}}_{\text{low-energy}} = \sum_{i=1,2}\Big[&-\hbar\Delta_i\hat{a}_i^\dagger\hat{a}_i + \hbar\omega_-\hat{c}_{i-}^\dagger\hat{c}_{i-}\\ &+\frac{\hbar\lambda}{\sqrt{N}}\left(\hat{a}_i^\dagger+\hat{a}_i\right)\left(\hat{c}_{i-}^\dagger\hat{c}_0+h.c.\right)\Big]\\ &+\frac{\hbar\lambda_{12}}{\sqrt{N}}\left(\hat{a}_1^\dagger\hat{a}_2+\hat{a}_2^\dagger\hat{a}_1\right)\left(\hat{c}_{12-}^\dagger\hat{c}_0+h.c.\right)\\ &+\hbar\omega_-\hat{c}_{12-}^\dagger\hat{c}_{12-}.\end{aligned} \tag{3}$$

We go to a mean-field description of this Hamiltonian by taking the average values $\langle\hat{a}_i\rangle = \alpha_i$

and $\langle \hat{c}_{i-} \rangle = \psi_i$ and $\langle \hat{c}_{12-} \rangle = \psi_{12}$. The mean-field Hamiltonian then becomes:

$$\begin{aligned} \mathcal{H}_{\mathrm{MF}} = \sum_{i=1,2} \Big[-\hbar\Delta_i\alpha_i^2 + \hbar\omega_-\psi_i^2 + \frac{4\hbar\lambda_i}{\sqrt{N}}\alpha_i\psi_i\psi_0 \Big] \\ + \frac{4\hbar\lambda_{12}}{\sqrt{N}}\alpha_1\alpha_2\psi_{12}\psi_0 + \hbar\omega_-\psi_{12}^2. \end{aligned} \tag{4}$$

Effective potential for the mixed phase To derive the Landau potential or free energy $\mathcal{F}$ that we show in the main text (see Fig. 4), we use the steady state solutions of the atomic fields ψ_i and ψ_{12} to reduce $\mathcal{H}_{\mathrm{MF}}$ to a function of the photon field amplitudes α_1 and α_2. Therefore we set $\partial\mathcal{H}_{\mathrm{MF}}/\partial\psi_i = 0$ and obtain $\psi_i = -2\lambda_i\alpha_i\psi_0/(\sqrt{N}\omega_-)$ for i=1,2 and $\psi_{12} = -2\lambda_{12}\alpha_1\alpha_2\psi_0/(\sqrt{N}\omega_-)$. The atomic fields respect the normalization condition $\psi_0^2 = N(1-\psi_1^2-\psi_2^2-\psi_{12}^2)$. Substituting these expressions into $\mathcal{H}_{\mathrm{MF}}$ and keeping terms up to quartic order in α_1 and α_2, we obtain the expression for the free energy:

$$\begin{aligned} &\mathcal{F}(\alpha_1, \alpha_2; r_1, r_2, g, \gamma_{12})/\hbar = \\ &\quad - \Delta_1\Big(1 - \frac{\lambda^2}{\lambda_{1,\mathrm{crit}}^2}\Big)\alpha_1^2 - \Delta_2\Big(1 - \frac{\lambda^2}{\lambda_{2,\mathrm{crit}}^2}\Big)\alpha_2^2 \\ &\quad + \frac{16\lambda^4}{\omega_-^3}(\alpha_1^2+\alpha_2^2)^2 - \frac{4\lambda_{12}^2}{\omega_-}\alpha_1^2\alpha_2^2 \end{aligned} \tag{5}$$

where we have set $\lambda_{i,\mathrm{crit}} = \sqrt{-\Delta_i\omega_-/4}$. This expression of the free energy is identical to the one presented in the main text where $r_i = -\Delta_i\Big(1 - \frac{\lambda^2}{\lambda_{i,\mathrm{crit}}^2}\Big)$, $g = 16\lambda^4/\omega_-^3$ and $\gamma_{12} = 4\lambda_{12}^2/\omega_-$. Note that the detuning imbalance is $\bar{\Delta} \equiv \Delta_2 - \Delta_1 = r_1 - r_2$. The phenomenology of the phase diagram, which is experimentally measured, can be reproduced by this free energy $\mathcal{F}$. Terms higher than the quartic order should be included to calculate the position of the phase boundary of the mixed phase. The ground state of the system for given parameters r_i, g and γ_{12} can be found by minimizing $\mathcal{F}$ with respect to both α_1 and α_2. In the case where $\gamma_{12} = 2g$, the free energy $\mathcal{F}$ separates,

$$\mathcal{F}(\alpha_1, \alpha_2; r_1, r_2, g, \gamma_{12})/\hbar = r_1\alpha_1^2 + g\alpha_1^4 + r_2\alpha_2^2 + g\alpha_2^4$$
$$= \mathcal{F}(\alpha_1; r_1, g)/\hbar + \mathcal{F}(\alpha_2; r_2, g)/\hbar.$$

In this case the phase boundaries of the two ordered phases SO1 and SO2 do not influence each other through the phase diagram as it is measured in Fig. 2**c** of the main text.

* esslinger@phys.ethz.ch

[1] Julian Léonard, Andrea Morales, Philip Zupancic, Tobias Donner, and Tilman Esslinger, "Monitoring and manipulating Higgs and Goldstone modes in a supersolid quantum gas," Science **358**, 1415–1418 (2017).

[2] Julian Léonard, Andrea Morales, Philip Zupancic, Tilman Esslinger, and Tobias Donner, "Supersolid formation in a quantum gas breaking a continuous translational symmetry," Nature **543**, 87–90 (2016).